

The Specialist Committee on Ice Final Report and Recommendations to the 29th ITTC



1. INTRODUCTION

1.1 Membership and meetings

The members of the Specialist Committee on Ice of the 29th International Towing Tank Conference are as follows:

1. Topi Leiviskä (Chair), Aker Arctic Technology inc, Finland
2. Franz von Bock und Polach (Secretary), Hamburg University of Technology, Germany
3. John Wang, National Research Council of Canada, Canada
4. Yinghui Wang, China Ship Scientific Research Centre (CSSRC), China
5. Nils Reimer, Hamburgische Schiffbau-Versuchsanstalt GmbH (HSVA), Germany
6. Yan Huang, Tianjin University, China
7. Takatoshi Matsuzawa, National Maritime Research Institute (NMRI), Japan
8. Aleksei Alekseevich Dobrodeev, Krylov State Research Centre (KSRC), Russia
9. Jinho Jang, Korea Research Institute of Ships and Ocean Engineering (KRISO), Korea
10. Pentti Kujala, Aalto University, Finland (Mikko Suominen 2017-2018)

Four Committee meetings were held as follows:

1. January 24 – 25, 2018, Helsinki. Participants: Leiviskä (Chair), von Bock und Polach (Secretary), Reimer, Dobrodeev, Suominen, Jang, J.Wang, Y.Wang, Matsuzawa. Absent: Huang.
2. June 14, 2018, Skype meeting. Attendance: Leiviskä (Chair), Matsuzawa, Jang, Reimer, Suominen, J.Wang, Dobrodeev. Absent: Huang, von Bock und Polach, Y.Wang.
3. November 21-22, 2018, Tianjin. Participants: all members, Leiviskä (Chair), von Bock und Polach (Secretary)
4. January 16-17, 2020, St John's Canada. Attendance: von Bock und Polach (Chair), Matsuzawa, Jang, Reimer, J.Wang, Dobrodeev, Kujala. (secretary) Absent: Leiviskä, Huang, Y.Wang.

2. MATERIALS

2.1 Terms of Reference

1. Continue to maintain, review and update existing accepted procedures and guidelines in accordance with current practice.
2. Review manoeuvring experiments in ice, and revise "7.5-02-04-02.3 Manoeuvring Tests in Ice" in cooperation with the Manoeuvring Committee.
3. Conduct survey of uncertainty in ice model experiments, and revise "7.5-02-04-02.5 Experimental Uncertainty Analysis for Ship Resistance in Ice Tank Testing."
4. Review of current analytical and numerical determination methods for the global ice load upon offshore structures of various types and compare to physical modelling.
5. Survey testing of platforms and monopiles in ice (such as wind turbine in frozen ocean) and consider establishing a new guideline or enhancing existing guidelines to cover such situation.
6. Update the Guideline 7.5-02-07-01.3 "Guidelines for Modelling of Complex Ice Environments" to cover additional complex conditions.

The tasks were divided into two groups. The committee decided to focus first on Tasks 1, 2, 3 and 6, and concentrate on Tasks 4 and 5 at later stage. A group leader was nominated to each task and group members were listed. Everyone had a possibility to join any of the groups.

3. UPDATES ON THE REVISED GUIDELINES

The following Guidelines were revised and updated. In addition to corrections and amendments the symbols in all Guidelines were reviewed and corrected follow the ITTC Symbols and Terminology List, Version 2017.

3.1 7.5-02-04-01 General Guidance and Introduction to Ice Model Testing

In this Guidelines there was only some minor spelling error corrections in Equations 1 and 2.

3.2 7.5-02-04-02 Test Methods for Model Ice Properties

In addition to spelling errors some corrections to the equations were made and, also one ice measurement method was added.

3.2.1 Correction of Equation 3 (Elastic modulus):

In Section 3 the definition of the Strain Modulus of Elasticity was faulty in Equation 3 and the exponent of thickness h was corrected from 2 to 3. The definition of the strain elasticity is:

$$E = \frac{3}{16} \frac{1-\nu^2}{kh^3} \left(\frac{F}{\delta}\right)^2 \quad (1)$$

where:

- F = loading force,
- g = gravitational acceleration,
- k = foundation factor ($k = g\rho_w$).

3.2.2 Correction of Equation 6 (characteristic length)

In section 3.1.3 where the Infinite Plate-Bending Method C with Larger Load Radius is presented, the square root was changed to the 4th root in Equation 6 in order to be correct:

$$l_c = \sqrt[4]{\frac{Eh^3}{12(1-\nu^2)w}} \quad (2)$$

3.2.3 Section 3.2: changing of wording:

The strain modulus – which can be elastic or elastic-plastic - can be determined by

cantilever beam tests and the use of the beam-bending differential equation.

The original wording was: “The elastic strain modulus can be determined by cantilever beam tests and the use of beam-bending differential equation”. The new wording is: The strain modulus – which can be elastic or elastic-plastic - can be determined by cantilever beam tests and the use of the beam-bending differential equation. The change of wording was done because purely elastic deformation cannot be stated with certainty for all cases.

3.3 Review manoeuvring experiments in ice, and revise "7.5-02-04-02.3 Manoeuvring Tests in Ice" in cooperation with the Manoeuvring Committee.

It was noticed that the previous guideline was very inadequate and in principle the whole document was re-written. It was also expected that the review will be done in cooperation with the Manoeuvring Committee.

The purpose of the procedure was defined: Definition of standards for performing manoeuvring tests in model ice. While manoeuvring test is a common name for all those tests in which the rudder is turned or the turning forces and moments are obtained by other means e.g. azimuthing thrusters or tunnel thrusters in bow. This procedure covers the most common manoeuvring tests for which standard methods exist in the different ice basins.

Typical manoeuvring tests in ice include turning circle tests, star manoeuvres and breaking out of channel. The model tests are often performed with a free model under its own propulsion. Sometimes, manoeuvring tests can be performed with a captive mode using x-y carriage or PMM (Planar Motion Mechanism). This allows force measurements, and it is mainly ad-hoc approach for certain cases.

The testing conditions of the model should be measured and documented similar as defined for Recommended Procedure for Free Running Model Tests 7.5-02-06-01. The loading condition of the model (draft fore/aft and GM) should be checked and documented. The GM should be as close as possible to the specified target value. If no value is specified, the actual value should be determined and reported. This value should at least be adjusted in a realistic range as full scale tests have revealed that the heeling angle of the ship has a large influence on the turning capability. For manoeuvring test with larger models at relatively low speed (e.g. turning circle) the correct adjustment of GM value is of lower relevance

3.3.1 Turning circle test

In turning circle tests which are one of the most common manoeuvring tests, mainly the test procedures were clarified as follows:

The purpose of the turning circle test is to find out how much area is needed to turn the ship. In practice, the result of this kind of test may look as shown in Figure 1.

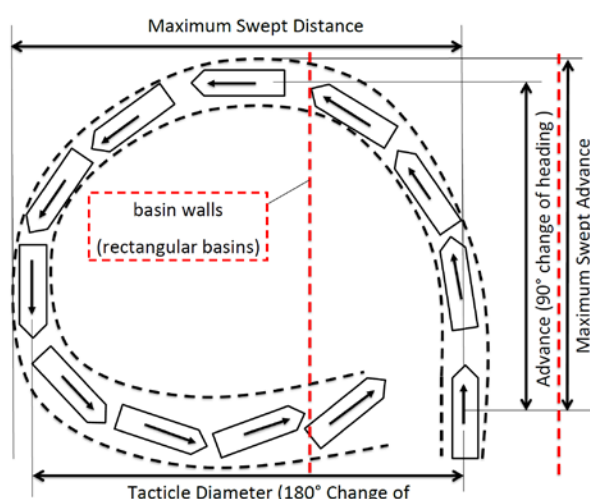


Figure 1: Definition of quantities used in turning circle tests

The test is started by proceeding the model straight ahead / astern at a certain speed into ice for at least one ship length. Thereafter a turning is induced by control of the rudder or thruster

angles. The turning is continued until the maximum possible turning angle (with respect to basin restrictions) is achieved.

If the turning diameter, D_c , or radius, R_c , is determined, the method by which it was obtained should be described. The turning circle may be not a perfect circle, but a spiral.

Because majority of ice model test basins are long and narrow, also the determination of the turning radius was clarified especially, when a 180 degree turning is not possible. There are also several error sources in turning tests which were brought out:

It should be noted that there are several error sources (e.g. channel width variation) when determining the turning radius based on a limited number of measured points and limited turning angle. The relative error of turning radius clearly decreases for higher achieved turning angles. The main reason is the aforementioned asymmetry of the turning track.

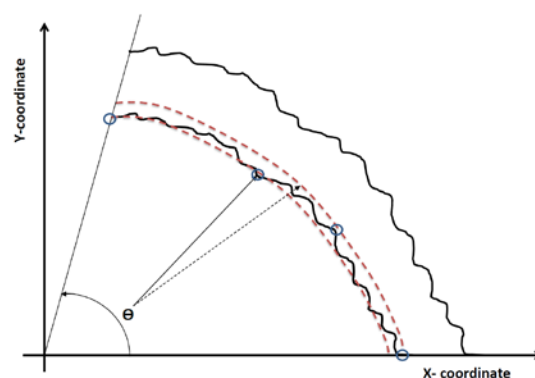


Figure 2: Broken channel of turning test

Considerable errors may appear, if the determination of D_c or R_c is based on a too small turn. Figure 2 presents an example of the broken track left after a turning circle test. To illustrate the possible maximum error in diameter D_{inn} , when determined based on few points on the inner circle, as a function of the turning angle.

In many cases motion capture data can be used to alternatively derive the turning radius from the time series of models change of heading.

3.3.2 Breaking out of channel test and star manoeuvre

Channel outbreking test and star manoeuvre were reviewed and in principle totally rewritten. The procedures of the channel outbreking test and star manoeuvre are written as follows:

Breaking out of channel is a test which can be performed from zero speed or some other specified speed. The model is typically accelerated to a certain speed or power in the channel and thereafter the rudder / azimuth thrusters are turned. The model will change heading and the fore or aft shoulders will break ice from the channel edges. After achieving a certain yaw angle the model will be able to enter the surrounding ice sheet (Figure 3). The test is concluded by leaving the channel completely (or at a specified yaw angle). The success of breaking out of channel manoeuvre is significantly affected by the width of the broken channel (in relation to model width).

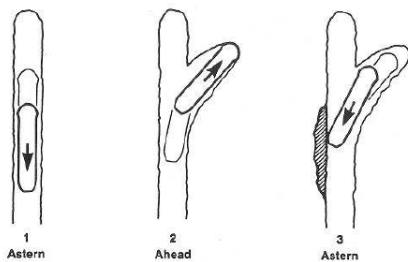


Figure 3: Sketch Break Out Manoeuvre, Quinton, Lau (2006)

The most relevant parameters that should be determined and reported are required distance in the channel (starting / end point), number of required attempts and time consumption.

Star Manoeuvre or Captain's turn is typically used when space and / or manoeuvring space is limited: The vessel turns

around 180 deg by performing a series of channel breakouts fore and aft (Figure 4).

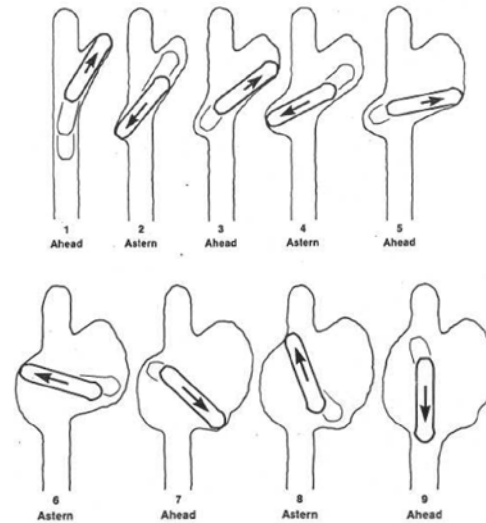


Figure 4: Sketch Star Manoeuvre, Quinton, Lau (2006)

Results to be obtained and reported for the star manoeuvre (captain's turn) are similar to those of break out tests.

3.3.3 Additional Comments which were added to the procedures

It should be noted that typically the behaviour of the model propulsion and manoeuvring / steering units does not exactly reflect the capability of the ships propulsion and manoeuvring systems. The reason is that stiffness and dynamic response of the model propulsion trains are not adjusted according to scaling similarities.

Further effects on manoeuvring tests resulting from restricted basin dimensions should be avoided.

As the results of manoeuvring tests are subject to the actual operating of manoeuvring systems the procedure for each manoeuvre should always be clearly documented and influence from operator should be limited to a minimum extent.

3.3.4 Cooperation with the Manoeuvring Committee

The task obligated also cooperation with the Manoeuvring committee. There were discussions between the committees on relevance of captive model test for ice, harmonization of general introduction and description of required data between 75-02-06-01 (open water) and 7.5-02-04-02.3 (ice) and frequent updates between the two committees on what is modified in the ice manoeuvring guideline. After all, it was found that common ground between the two groups is limited, but cooperation and exchange will continue.

3.4 Conduct survey of uncertainty in ice model experiments, and revise "7.5-02-04-02.5 Experimental Uncertainty Analysis for Ship Resistance in Ice Tank Testing."

This task was not completed as planned. There are several uncertainty sources in ice model testing, some of which are not very well recognized. Most of the sources are related to ice properties. However, the following actions were taken for this task: Ice resistance test results using 4 ice sheets were used for the ITTC's present uncertainty analysis. For each ice sheet, two channels with three speeds were tested and 18 in-situ cantilever beam tests for each channel were performed. Ice resistance uncertainty as well as ice flexural strength uncertainty was investigated. Review of current analytical and numerical determination methods for the global ice load upon offshore structures of various types and compare to physical modelling.

3.5 Review of current analytical and numerical determination methods for the global ice load upon offshore structures of various types and compare to physical modelling.

Piled structures in ice

Prepared by Yan Huang

Piled structures in arctic and cold regions shall have the abilities to resist ice actions. Such structures generally include single pile structures (e.g., monopile foundations for offshore wind farms) and multi-pile structures (e.g., offshore jacket platforms, or multi-leg foundations for docks and wind turbines). Regarding single pile structures, global ice loads, ice induced vibrations and scaling methods for ice model testing are the key issues studied for many years. For multi-pile structures, influences of interference and sheltering effects, non-simultaneous failure, ice jamming and rubble building on global ice loads are the main topics in the published research programs.

1. Single pile structure

1.1. Global ice load

The global ice loads for single pile structures have been widely studied by many scholars through field observations, model tests and mathematical analyses, and several design formulas have been proposed. Despite the differences in the detailed expressions of the formulas, the global ice loads are generally treated as a function of ice thickness h , structural width w and ice strength σ_c . For now, the most applicable formula may be the ISO algorithm (ISO 19906, 2010) expressed as:

$$F_G = p_G \cdot h \quad (3)$$

$$p_G = C_R \cdot (h/h_1)^n \cdot (w/h)^m \quad (4)$$

where F_G is the global ice action normal to the surface, in MN; p_G is the global average ice pressure, in MPa; w is the projected width of the structure, in m; h is the thickness of the ice sheet, in m; h_1 is a reference thickness of 1 m; m is an empirical coefficient equal to -0.16 ; n is an empirical coefficient equal to $-0.50 + h/5$ for $h < 1.0$ m, and to -0.30 for $h \geq 1.0$ m; C_R is the ice strength coefficient, in MPa.

The ISO algorithm considered the size effect in the ice pressure and obtained full-scale measurements data from Cook Inlet, Beaufort Sea, Baltic Sea and Bohai Sea. The ISO formulas have also been adopted by several design rules or guidelines in their latest versions, such as the API RP 2N (API, 2015) and the DNV OS J101 (DNV, 2014).

It should be noted that the Eq. (3) and Eq. (4) apply only for rigid structures and do not take into account the effects of ice-induced vibrations, which can arise in compliant structures.

1.2. Ice induced vibration

When ice breaks up, static and dynamic interactions will take place between the structure and the ice. For compliant structures, the natural vibrations of the structure will affect the break-up frequency of the ice, such that it becomes tuned to the natural frequency of the structure. This phenomenon is known as lock-in and implies that the structure becomes excited to ice induced vibrations in its natural mode shapes. The structure shall be designed to withstand the loads and load effects from dynamic ice loading associated with lock-in when ice induced vibration occurs.

There have been divergences on the mechanism that controls the procedure of ice induced vibrations on vertical structures. Some scholars such as Peyton (1968) and Neil (1976) have the opinion that steady state vibration caused by ice is a resonant vibration that relates to a concept known as the failure length of ice. Similar conclusions were obtained in field and lab tests by Michel (1978), Sodhi and Morris (1986) and Sodhi (2001). They reported that that the failure frequency of ice is directly proportional to ice velocity and inversely proportional to ice thickness. Resonant vibration may arise when the failure frequency is close to the natural frequency of the structure.

Other scholars took the interaction between ice and a flexible structure as the control

mechanism of the procedure of ice induced steady vibration. Basing on the field observation in Kulk gulf, Matlock et al. (1969) established a numerical model on the consideration of the displacements and elastic deformations of ice sheet and structure. Some scholars hold the viewpoint that the break size of ice is controlled by structure, and the cause of ice induced vibration is the negative damping factor engendered in course of ice-structure interaction (Määttänen, 1977). Subsequently, this consideration was developed into the self-excited vibration theory, which is supported by quite a few scholars. On the basis of self-excited vibration theory, Yue (2004) analysed the problem from a new aspect that considered the material characteristics of ice and the feedback effect of the structure response. Some scholars also analysed the problem from the aspect of energy transition (Kärnä and Turunen, 1989, 1990).

Based on a series of single pile tests, Huang et al. (2007) established an interaction coefficient I (Eq. 5) to account for the influences of structure stiffness, natural frequency of the structure, ice elasticity and ice speed on the ice-structure interaction and evaluate the response level of the structure under dynamic ice loading:

$$I = -\ln K / Eh \cdot \ln (Df_0) / V \cdot D / h \quad (5)$$

where K is the structure stiffness; E is the elastic modulus of ice; h is the ice thickness; D is the structural width; f_0 is the natural frequency of the structure; V is the ice drift speed. Based on the interaction coefficient I , Huang et al. (2007) proposed a range of 20–45 for the identification of violent ice induced vibrations. This range was later valid by field observation and multi-pile tests (Huang et al., 2013).

1.3. Scaling for ice model testing

The traditional Froude and Cauchy scaling approach for ice model testing is originated in the scaling of ships breaking ice (ITTC, 2017). Such approach is considered to be valid when

the material behavior of the ice can be treated as linear elastic and inertia forces are significant under high speeds during ship-ice interaction.

For the interaction with pile structures, ice can fail in various ways, leading to the questioning on the applicability of Froude and Cauchy similarities. As known, the strength of the ice depends on the grain structure, temperature, degree of confinement and the loading rate, resulting in different behaviours of ice failure including creep, viscoplasticity, elasticity, or plasticity (Timco, 1987). Thus, in the interaction between a pile structure and a floating ice sheet, the ice may fail in creep, crushing, buckling, bending, etc.

Many investigators have conducted small-scale and medium-scale indentation tests to understand the ice crushing process, and the effects of indentation speed on the mode of crushing failure have been identified: creep deformation of ice at low speed, intermittent crushing against compliant structures at intermediate speeds, and continuous brittle crushing at high speeds (Sodhi et al., 1998). Sodhi (2001) presented a map of ice crushing failure during interactions with rigid and compliant structures (see Figure 5) and pointed out the existences of one transition speed (i.e., ductile to brittle) for rigid structures, and two transition speeds (i.e., ductile to intermittent and intermittent to brittle) for compliant structures. Huang et al. (2007) found that the two transition speeds for compliant structures are not constant but changing with different structure stiffness values.

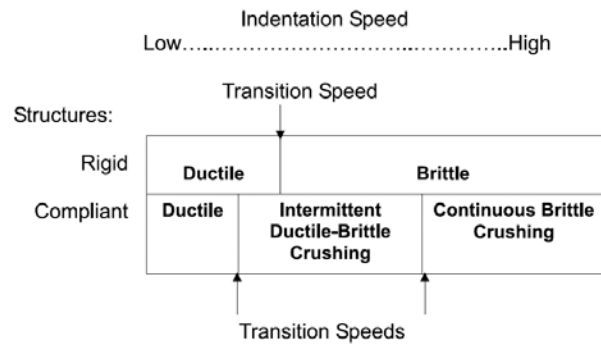


Figure 5: Ice crushing failure mode in terms of indentation speed and type of structure (Sodhi, 2001)

Therefore, in the application of Froude-Cauchy scaling for the interaction between ice and pile structures, the following issues need to be addressed:

i. The transition interaction speed or loading rate for the definition of the elasticity for ice, which determines the applicability of Cauchy scaling. Derradji-Aouat (2003) proposed that ice behaves as a linear elastic material with a brittle mode of failure at high-speed impacts where the strain rates are higher than 10^{-3}s^{-1} . Such threshold was obtained from triaxial tests (Derradji-Aouat, 2000) and can be applicable for rigid structures. For compliant structures, however, the two transition speeds are difficult to define with structural stiffness involved. Based on the interaction coefficient I , Huang et al. (2007) proposed a range of 20–45 for the identification of violent ice induced vibrations, but the link between violent structural response and ice failure modes (i.e., intermittent ductile-brittle or continuous brittle) still needs to be clarified on the basis of specific structural dynamic characteristics.

ii. Alternative scaling methods for the ductile and intermittent ductile-brittle failure of ice. The Froude-Cauchy scaling is inapplicable for pile structures under low ice drift speed as the ice may fail in ductile or intermittent ductile-brittle mode and the inertia forces are small. As von Bock und Polach and Molyneux (2017) stated, specific similarities need to be developed for each single case (scenario), and the case-based scaling is considered more

practical than the definition of one global scaling approach. Atkins and Caddell (1974) developed a non-dimensional ice number In to maintain both the Froude law and the cracking law, but the application of the In is still in the brittle regime. For small-scale laboratory tests on ice moving slowly against structures, Palmer and Dempsey (2009) proposed that the Froude scaling is unnecessary and can be abandoned and developed a dimensionless group lW/E (l is the characteristic length of the system, E is the elastic modulus and W is the weakening rate) based on nonlinear fracture mechanics to maintain the same notch sensitivity as the prototype, which inferred that the best material to model sea ice is the real saline ice itself, and artificial reduction of strength was not suggested. The suggestion of using real saline ice is consistent with the concept of replica modelling proposed by Sodhi (1998), but the latter is used for brittle crushing during edge indentation of ice sheets at high speeds.

iii. The elasticity of model ice. Recently, von Bock und Polach et al. (2013) found that model ice is not a linear elastic material, even at strain rates above 10^{-3}s^{-1} , and the model ice could be rather represented by strain modulus than elastic modulus. Thus, for the application of the Cauchy scaling, studies are still needed to reduce the plasticity of the model ice and increase its stiffness.

2. Multi-pile structures

Differential and multi-directional ice actions on multi-pile structures shall be considered in design, and the accuracy of determining the ice load is of ultimate importance since it directly influence the operational safety and cost.

Studies concerning the ice actions on multi-pile structures are mainly from laboratory tests. According to the ISO 19906 (2010), the global ice load on a multi-leg structure can be defined as follows:

$$F_S = k_s k_n k_j F_l \quad (5)$$

where k_s accounts for the interference and sheltering effect; k_n accounts for the effect of non-simultaneous failure; k_j accounts for the ice jamming; F_l is the ice force on one leg that is not influenced by the above effects.

2.1. Interference and sheltering effect

When ice interacts with pile-groups, the ice failure mechanism and the ice load tend to alter when the lateral pile spacing is less than a certain value, which is commonly known as interference effect. On the other hand, the sheltering effect is that the ice sheet will first contact and mostly failed in the front piles when interacted with pile groups, leading to a reduction of the ice force on the back piles, and the value of k_s can be studied by the above two factors. In works of Kato and Sodhi (1984) and Saeki and Ono (1986), the interaction between multi-piled structure and ice sheet can be mainly studied in two modes:

- i. The line connecting the adjacent piles is perpendicular to the ice moving direction.
- ii. There is a certain angle between the line connecting two adjacent piles and the ice moving direction.

For the first interaction mode, the interference effect is significantly influenced by the lateral pile spacing L in the front row of legs. If this distance is large, each leg interacts with the ice sheet independently of the other legs. In this case, the sheltering factor, k_s , approaches the number, n , of the legs. Where all legs are on a line perpendicular to the drift direction, data from limited model tests suggest that the legs act independently of each other if the ratio of the clear distance, L , between the legs and the width, w , of an individual leg is greater than 5. Field evidence from the Confederation Bridge suggests some interaction between piers for L/w ratios of about 10. For a typical multi-leg structure where the legs are not in a single line, the legs become independent at a higher value of L/w .

For a typical multi-leg structure with four legs, the maximal sheltering factor varies from 3.0 to 3.5. But it should be mentioned that this is mainly for four leg structures, which maybe not suitable for other multi-piled structures.

For the second mode, the angle of incidence of the ice drift influences the ice action. Some guidance on the distribution of loads between legs for multi-leg structures based on model tests can be found in Wessels and Kato (1988). Li et al. (2017) also performed a series of model tests to evaluate the interference and sheltering effect, and an integrated reduction coefficient was introduced to describe these effects.

2.2. Non-simultaneous effect

Non-simultaneous failing effect tends to affect the ice loads and failure mechanisms for the multi-leg structures. Observations of non-simultaneous crushing failure of ice were proposed by several researchers on wide structures, on which appears several independent crushing zones during the ice failure process on wide vertical walls or cones (Kry, 1978; Kry, 1980; Kamesaki et al., 1997; Takeuchi, 1999). Jordaan (2001) developed the concept “independent zones” as “high-pressure zones” and studied the distributions of the hpz. Huang (2010) conducted a series of model tests to observe the ice bending failure before wide conical and pointed out the failures of ice wedges around the cone start to behave non-simultaneously when $D/h > 25$ (D is the waterline diameter and h is the ice thickness).

For multi-pile structure, the non-simultaneous effect exists with similar but more complicated mechanism, and published studies mainly focus on the value of k_n when piles directly interact with the ice sheet. Kato et al. (1994) carried out a series of research works on multi-legged structure with vertical piles. It is noticed that non-simultaneous failure also caused the decreasing of ice loading, but the effect of non-simultaneous factor is not extensive discussed because of the insufficient test data, and the coefficient was recommended

as 1.0. Shi et al. (2002) gave experimental investigations on the non-simultaneous failure of ice for two in a row and five piles in a row, respectively. The results showed that the k_n can be taken as 0.875 for two piles and 0.774 for five piles. ISO 19906 (2010) recommended 0.9 for the value of k_n but also mentioned such value is estimated with the absence of test data. Li et al. (2017) performed a series of model tests to investigate the maximum ice loads on a multi-pile structure with slightly sloping piles and found that the non-simultaneous failure of ice becomes more complicated in comparison with the vertical ones. This can be attributed to the mixed failure mode observed in the tests with the flexural failure of ice resulting in different loads than the normal compressive failure.

2.3. Ice jamming and rubble building

Ice jamming between the legs can be expected if L/w is less than 4. Huang et al. (2017) observed severe ice jamming between the conductor array of a jacket platform in Bohai Sea and carried out a series of model tests to investigate the ice pile-up process within the conductor array and the ice load acting on it. According to the ISO 19906 (2010), ice jamming may lead to an increase in the ice action. Results from Huang et al. (2017) agreed with such point of view, but also indicted a reduced R when using the ISO algorithm (Eq. 6 and Eq. 7) to calculate the horizontal ice load acting on the conductor array due to ice rubble building in front of the structure.

$$F_B = p_D D \quad (6)$$

$$p_D = R h^{1.25} D^{-0.54} \quad (7)$$

where F_B is the horizontal ice force due to rubble building, in MN; p_D is the rubble building action per unit width, in MN/m; R is a coefficient; h is the ice thickness, in m; D is the width of the ice feature, in m.

Where there is any chance that ice can jam between the legs, both the jammed and

unjammed cases should be considered, and the maximum value of ice action selected.

References

- ISO 19906, 2010. Petroleum and natural gas industries—Arctic offshore structures. International Organization for Standardization, Geneva.
- API, 2015. Planning, Designing, and Constructing Structures and Pipelines for Arctic Conditions. ANSI/API Recommended Practice 2N Third Edition, American Petroleum Institute.
- DNV, 2014. Design of Offshore Wind Turbine Structures. Offshore Standard DNV-OS-J101, Det Norske Veritas.
- Peyton, H.R., 1968. Sea ice Forces. Ice pressure against structures. Technical Memorandum, vol. 92. National research Council of Canada, Ottawa, Canada, pp. 117–123.
- Neil, C.R., 1976. Dynamic ice forces on piers and piles: an assessment of design guidelines in the light of recent research. Canada journal of civil engineering, vol. 3, pp. 305–341.
- Michel, B., 1978. Ice Mechanics. Laval University Press, Quebec, P.Q., Canada, pp. 298–299.
- Sodhi, D., Morri, C.E., 1986. Characteristic frequency of force variations in continuous crushing of sheet ice against rigid cylindrical structures. Cold regions Science and Technology, vol. 12, pp. 1–12.
- Sodhi, D.S., 2001. Crushing failure during ice–structure interaction. Engineering Fracture Mechanics 68, 1889–1921.
- Matlock, H., Dawkins, W., Panak, J., 1969. A model for the prediction of ice–structure interaction. Proc. 1st Offshore Tech. Conf., Houston, OTC 1066, vol. 1, pp. 687–694.
- Määttänen, M., 1977. Stability of self-excited ice-induced structural vibration. Proceedings of 4th International Conference on Port and Ocean Engineering under Arctic conditions (POAC), vol. 2. St. John's Newfoundland, Canada, pp. 171–176.
- Yue, Q.J., 2004. Crushing formed dynamic ice loads during interacting with vertical compliant structure. Engineering Mechanics 2, 200–208.
- Kärnä, T., Turunen, R., 1989. Dynamic response of narrow structures to ice crushing. Cold Regions Science and Technology 17, 173–187.
- Kärnä, T., Turunen, R., 1990. A straightforward technique for analysing structural response to dynamic ice action. Proceedings of the 9th International Conference of Offshore Mechanics and Arctic Engineering, vol. 4, pp. 135–142.
- Huang, Y., Shi, Q.Z., Song, A., 2007. Model test study of the interaction between ice and a compliant vertical narrow structure. Cold Regions Science and Technology 49, 151–160.
- Huang, Y., Yu, M., Tian, Y.F., 2013. Model tests of four-legged jacket platforms in ice: part 2. Analyses and discussions. Cold Reg. Sci. Technol. 95, 86–101.
- ITTC, 2017. General Guidance and Introduction to Ice Model Testing. ITTC Recommended Procedures and Guidelines, International Towing Tank Conference.
- Timco, G.W., 1987. Indentation and penetration of edge-loaded freshwater ice sheets in the brittle range. Journal of Offshore Mechanics & Arctic Engineering, 4(3), 287–294.
- Sodhi, D.S., Takeuchi, T., Nakazawa, N., Akagawa, S., Saeki, H., 1998. Medium-scale indentation tests on sea ice at various speeds. Cold Reg. Sci. Technol. 28, 161–182.

Derradji-Aouat, A., 2003. Multi-surface failure criterion for saline ice in the brittle regime. *Cold Regions Science and Technology* 36: 47–70.

Derradji-Aouat, A., 2000. A unified failure envelope for isotropic freshwater ice and iceberg ice. ASME/OMAE-2000, Int. Conference on Offshore Mechanics and Arctic Engineering, Polar and Arctic section, New Orleans, US.

von Bock und Polach, R.U.F., Molyneux, D., 2017. Model ice: A review of its capacity and identification of knowledge gaps. *Proceedings of the ASME 2017 36th International Conference on Ocean, Offshore and Arctic Engineering (OMAE2017)*, Trondheim, Norway.

Atkins, A.G., Caddell, R.M., 1974. The laws of similitude and crack propagation. *International Journal of Mechanical Sciences*, 16(8): 541–548.

Palmer, A., Dempsey, J., 2009. Model tests in ice. *Proceedings of the 20th International Conference on Port and Ocean Engineering under Arctic Conditions*, Luleå, Sweden.

Sodhi, D.A., 1998. Nonsimultaneous crushing during edge indentation of freshwater ice sheets. *Cold Regions Science and Technology* 27: 179–195.

von Bock und Polach, R., Ehlers, S., and Kujala, P., 2013. Model scale ice - part a: Experiments. *Cold Regions Science and Technology*, 94: 53–60.

Kato, K., Sodhi, D.S., 1984. Ice action on two cylindrical structures. *Journal of Energy Resources Technology*, 106: 107-112.

Saeki, H., Ono, T., 1986. Total ice forces on the clusters of cylindrical piles. In: 5th OMAE international conference on offshore mechanics and Arctic engineering, Tokyo, Japan.

Wessels, E., Kato, K., 1988. Ice Forces on Fixed and Floating Conical Structures, *Proc. 9th IAHR Int. Symp. on Ice*, Sapporo, Japan.

Li, W., Huang, Y., Tian, Y., 2017. Experimental study of the ice loads on multi-piled oil piers in Bohai Sea. *Marine Structures*, 56: 1-23.

Kry, P.R., 1978. A statistical prediction of effective ice crushing stress on wide structure. *Proc. 4th IAHR Symposium on Ice Problems*, Lulea, Sweden, pp. 33–47.

Kry, P.R., 1980. Third Canadian geotechnical colloquium: Ice force on wide structures. *Canadian Geotechnical Journal*, 17(1):97-113.

Kamesaki, K., Tsukuda H., Yamauchi, Y., 1997. Experimental studies on non-simultaneous failure characteristic of vertical sided indentors. In: 7th ISOPE international offshore and polar engineering conference. Honolulu, USA.

Takeuchi, T., 1999. Indentation pressure in ice/structure interaction based on statistical generation of ice failure surface. *Proceedings of the international offshore and polar engineering conference*, 2: 505-511.

Jordaan, I.J., 2001. Mechanics of ice-structure interaction. *Engineering Fracture Mechanics* 68, 1923–1960.

Huang Y., 2010. Model test study of the nonsimultaneous failure of ice before wide conical structures. *Cold Regions Science and Technology*, 63(3): 87-96.

Kato, K., Adachi, M., Kishimoto, H., Hayashinguchi, S., 1994. Model experiments for ice forces on multi conical legged structures. In: 4th ISOPE international offshore and polar engineering conference, Osaka, Japan.

Shi, Q., Huang, Y., Song, A., Tong, J., 2002. Non-simultaneous failure of ice in front

of multi-leg structures. China Ocean Engineering, 16:183-92.

Huang, Y., Sun, J., Wan, J., Tian, Y., 2017. Experimental observations on the ice pile-up in the conductor array of a jacket platform in Bohai Sea. Ocean Engineering, 140, 334-351.

3.6 Survey testing of platforms and monopiles in ice (such as wind turbine in frozen ocean) and consider establishing a new guideline or enhancing existing guidelines to cover such situation

The Technical Committee stress that the future procedure should include all stationary structures, including dynamic positioning in ice. Recently, very few tests have been conducted on this topic as the oil extrapolation in icy waters has practically stopped and the guideline might be outdated for the beginning. Therefore, the TC suggested just to write an outline for the future procedure. The outline is presented below:

Tests for Fixed Structures in Ice

- 1 PURPOSE OF PROCEDURE
- 2 TEST FOR FIXED STRUCTURES IN ICE
 - 2.1 Ice load tests for pile foundation structures
 - 2.2 Ice load tests for shallow foundation structures
 - 2.3 Ice induced vibration tests
- 3 PARAMETERS
 - 3.1 Parameters to be measured
 - 3.2 Ice parameters to be measured
- 4 VALIDATION
 - 4.1 Uncertainty analysis
 - 4.2 Benchmark tests
- 5 REFERENCES

3.7 Update the Guideline 7.5-02-07-01.3 “Guidelines for Modelling of Complex Ice Environments” to cover additional complex conditions.

The group leader for this task was Alexey Dobrodeev. Guidelines for Modelling of Complex Ice Environments was earlier transferred for some reason under 7.5-02-07-01 Environmental Modelling. However, Ice committee asked that the same time the guideline was updated it would also be transferred back under 7.5-02-04 Ice Testing. The reason was that the development of ice environments and conditions should be in hands of Ice Committee because these features are typically only used in ice model testing of ships or structures.

Two chapters were added to the guidelines. They were Compressive ice and Snow-Cover ice. The other chapters were updated to correspond to the current practices.

4. COMPRESSIVE ICE

4.1 Background

The term compression in an ice cover refers to a situation where wind and/or current exert drag force on ice cover and the ice starts to drift. When wind drag acts on open pack ice, the ice floes start to move. If the ice motion is restricted by an obstacle like a shoreline, the ice cover starts to compact. First all the open water area closes. This is followed by rafting of ice at the contact points between ice floes. The rafting is followed by ridging. When the force required to ridging is larger than the driving forces, the ice drift stops and stresses i.e. compression in the immobile ice cover will be present.



Figure 6: A ship stuck in compressive ice

There is a definite relationship between the compression level the closing speed of the channel (Sazonov, 2010) on the basis of the full-scale tests processing, which can be presented as approximation:

$$V_c = 0,005S_{IC} + 0,03762S_{IC}^2 \quad (8)$$

where V_c - the closing speed of the channel in m/s; S_{IC} – ice compression level measuring in numbers from 0 to 3. An ice compression from 0 to 3 on this scale can be described as:

0 – The ice is not compressed. There are channels, unclosed cracks and patches of ice-free water among the close ice.

1 – The ice is weakly compressed. In the compression zone separate patches of ice-free water and fresh cracks are observed. The brash ice between the ice floes is consolidated. There are rafted nilas and grey ice. There ice ridges among grey/white ice.

2 – The ice is distinctly compressed. In the compression zone only a few small patches of ice-free water and narrow cracks of variable width are preserved. This is an evidence of ice drift. The brash ice is partly extruded onto the ice channel edges. Fresh ice ridges are observed.

3 – The ice is strongly compressed. Open water and cracks are completely absent. Young ice is

completely formed into ridges. The brash ice is completely extruded onto/under the ice channel edges. The channel is closed behind the icebreaker at once. There are ice ridges at the junctions of first- and multi-year ice.

4.2 Method for modelling compressive ice

An ice feature approximating a natural rubble field can be created by compressing ice floes within the tank, into a single- or multi-layered rubble field. The steps in this method are as follows:

The tests are performed with a self-propelled model or by towing the model across the basin. A ship model is driven or pulled through an open channel and one side of the ice field is pushed perpendicular towards the heading of the model (Figure 7). The model can be towed by a carriage only if both side of ice can compress the model symmetrically. The compression level is determined based on the closing speed of the channel in relation to the ship speed.

Added resistance in relation to the level ice resistance and open channel resistance determined with tests in these features without a compression.

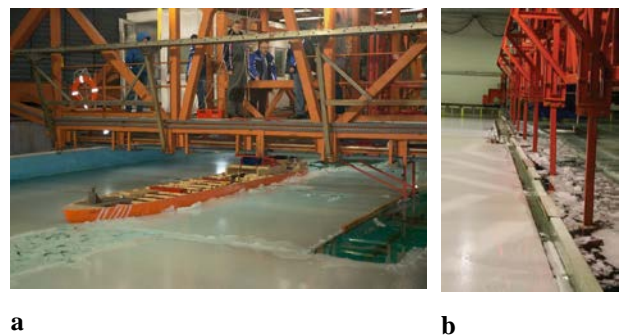


Figure 7: Towing tests of ship in compressive ice (a – the model towing with a winch across the KSRC basin during the pushing of ice sheet; b – the pushing plates lowered to the water level in AALTO basin)

4.3 Experiments and Testing

Resistance and propulsion tests can be performed in compressive level ice and closing channel see 7.5-02-04-02.1 “Resistance Test in Ice” and 7.5-02-04-02.2 “Propulsion Test in Ice”.

5. SNOW-COVERED ICE

5.1 General

Snow cover can have a significant effect on ice resistance and can increase the friction on a vessel's hull. It also provides an easily compressible layer, which consumes energy prior to fracturing the underlying ice, and entraps air which increases the buoyancy component. Such effects have been demonstrated through full-scale trials and model tests.

The results of full-scale sea trials provide conclusive evidence that snow cover on ice has significant effect on the ship's ice resistance. Typically, this effect is taken into account by assuming some effective ice thickness so that the ship's resistance in this effective ice thickness is equal to that in ice covered with snow.

5.2 Preparation

There are 3 approaches that could be used for preparing snow in model basin: modelling as an additional thickness to the ice sheet, artificially generating snow in basin (Huang 2018) and imitation by special chemical composition.

A so-called effective ice thickness h'_I , which is commonly introduced to include the snow effect on the ship's performance in ice, is defined as the ice thickness h_I plus some allowance for the snow-covered ice properties, primarily snow thickness h_{SN} . In this case it is assumed that the ice resistance of ship moving through continuous snow-free ice of thickness

h'_I is equal to the ice resistance of the same ship moving through snow-covered ice of thickness h_I plus snow thickness h_{SN} . Calculations are performed using the following formula:

$$h'_I = h_I + k_e h_{SN} \quad (9)$$

where k_e is a certain empirical coefficient.

Different researchers suggested different values for this coefficient k_e based on scanty results obtained in full-scale trials. According to Ref. (Buzuev A.Ya., 1981) based on the analysis of the studies conducted by various researchers the values of this coefficient are in the range of 0.5 to 1.5, while A.Ya. Buzuev suggested it's equal to 1. Alternative suggestion was made by (Nyman, 1999 & Riska, 2001) to use a value of k_e equal to 1/3. For a fresh snow cover this coefficient could be assumed to be $k_e = 0$ (Belyashov, 2008 & Appolonov, 2011).

In Ref. (Ryvlin, Heisin, 1980), also based on full-scale results, it is shown that the value of this coefficient should depend on the snow density. These authors suggested the following formula for k_e :

$$k_e = k'_e \frac{\rho_{SN}}{\rho_I} \quad (10)$$

where ρ_{SN}, ρ_I – snow and ice density, respectively; k'_e - empirical coefficient (in the opinion of the authors, equal to 4.2 for icebreakers). The authors used the linear dependence as the first approximation. This dependence is apparently applicable to snow densities up to 400 kg/m³.

The semi-empirical approach was further developed in Ref. (Gramuzov, 2011) that suggested the following formula for estimation of the coefficient k_e in Eq. (10):

$$k_e = 0.284 + 0.575 \cdot 10^{-3} S_{WB} - 0.164 h_I - 0.048 V \quad (11)$$

where V – ship speed, S_{WB} – wetted bottom area, m^2 .

This formula was derived based on numerical calculations of the ship's ice resistance using the method of B.P. Ionov and E.M. Gramuzov (Ionov, 2001). In these calculations the snow thickness h_{SN} and some initial ice thickness h_I were assumed. The resistance due to snow-covered ice was calculated based on the data of Ref. (Gramuzov, 1986). Then the effective ice thickness h'_I was calculated to meet the equal resistance condition.

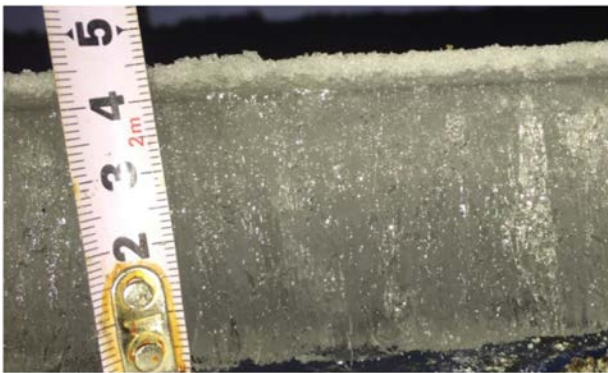


Figure 8: Artificially produced middle layer of depth hoar on model ice sheet (Huang, 2018)

The technique of artificially generating snow included in this method is forcing water vapour flowing over a cold snow surface to accelerate the formation of coarse-grained snow ice. A layer of snow ice is firstly produced on the model ice sheet by performing the two-order water pulverization procedure. Then a layer of coarse-grained snow ice with big crystal size (2–3 mm) is made by spraying the water vapour on the surface of new snow layer directly. As the wet snow particles are completely refrozen, another new snow layer is sprayed on this base layer subsequently. In the next step, water vapour is driven to horizontally flow over the new snow surface to accelerate the formation of depth hoar (Figure 8). Then a layer of dense and close-grained depth hoar is quickly developed on the base snow ice layer. The last step of the layered snow cover generation is spraying a layer of

new snow over the middle layer of depth hoar (Huang et al, 2016).

5.3 Experiments and Testing

Resistance and propulsion tests can be performed in snow cover ice see 7.5-02-04-02.1 “Resistance Test in Ice” and 7.5-02-04-02.2 “Propulsion Test in Ice”.

References

Appolonov, E.M., Belyashov, V.A. et al., 2011, “The Ice performance researching of icebreaker “Sankt-Peterburg” in the Kara Sea”, Sudostroenie, Issue 4, pp 9 - 12.

Belyashov, V.A., Sazonov, K.E. et al., 2008, “Yury Topchev” and “Vladislav Strizhov” multipurpose ice-breaking vessels for Prirazlomnaya platform maintenance: field and model tests. Proceedings of International Conference and Exhibition on Performance of Ship and Structures in Ice 2008”, ICETECH 2008, pp 105 - 113.

Buzuev, A.Ya., 1981, “Influence of environmental conditions on ship navigation in ice-covered waters”, Hydrometeoizdat, Leningrad, 200 p (in Russian).

Eriksson, P. et al., 2009. Research Report No 59, Helsinki: Winter Navigation Research Board.

Finnish Transport Safety Agency (TraFi) (2010), ICE CLASS REGULATIONS 2010 FINNISH-SWEDISH ICE CLASS RULES 2010, TRAFI/31298/03.04.01.00/2010.

Finnish Transport Safety Agency (TraFi) and Swedish Transport Agency (2011), GUIDELINES FOR THE APPLICATION OF THE FINNISH-SWEDISH ICE CLASS RULES, TRAFI/21816/03.04.01.01/2011.

Frederking, R and Timco, G., 1983, “On measuring flexural properties of ice using cantilever beams”, Annals of Glaciology 4.

Gramuzov, E.M., 1986, “Snow resistance of moving icebreaker”, The design of tools for navigation extension: interuniversity collection, Gorkovskiy politechnical institution, Gorkiy, pp 59 - 71. (in Russian).

Gramuzov, E.M., Tikhonova, N.E., 2011, “The method of taking account of snow on icebreaker resistance by means of present thickness of level ice sheet”, The proceedings of Nizhniy Novgorod State Technical University n.a. R.E. Alekseeva, Issue 4(91), pp 178 - 183.

Hamilton, J., Holub, C., et al., 2011, “Ice Management for Support of Arctic Floating Operations”, In Proc. of the Arctic Technology Conference.

Huang, Y. et al., 2018, “Experiments on navigating resistance of an icebreaker in snow covered level ice”, Cold Regions Science and Technology, Issue 152 (2018), pp 1 - 14.

Ionov, B.P., Gramuzov, E.M., 2001, “Ships ice performance”, Sudostroenie, St. Petersburg, 512 p (in Russian).

Tuhkuri, J., and Lensu, M., “Laboratory tests on ridging and rafting of ice sheets”, J. Geophys. Res., Issue 107(C9), 3125.

Leppäranta, M. and Hakala, R., 1992, “The structure and strength of first-year ice ridges in the Baltic”, Cold Regions Sciences and Technology, Volume 20, pp 295 - 311

Molyneux, D. and Spencer D., 2013, “Predicting Ice Loads on Offshore Structures”, Proceedings, 18th Offshore Symposium, Texas Section, SNAME, Houston, February 7.

Nyman, T., Riska, K. et al., 1999, “A. The ice capability of the multipurpose icebreaker Botnica – full scale results”, POAC 99, Espoo, Finland, Volume 2, pp 631 - 343.

Prodanovic, A., 1979. “Model tests of ice rubble strength. Proc. Port and Ocean Engineering under Arctic Conditions”, The

University of Trondheim, The Norwegian Institute of Technology, Trondheim, Norway, pp 89 - 105.

Riska, K., Leiviskä, T. et al., 2001, “Ice performance of the swedish multi-purpose icebreaker Tor Viking II”, POAC 01, Ottawa, Ontario, Canada, Volume 2, pp 849 - 866.

Ryvlin, A.Ya., Heisin, D.E., 1980, “Ship ice trials”, Sudostroenie, Leningrad, 208 p (in Russian).

Sazonov, K. E., 2010, “Theoretical principles of ship navigation in ice”, Krylov Shipbuilding Research Institute, St. Petersburg, Russia, 274 p.

Strub-Klein, L., and Sudom, D., 2012, “A comprehensive analysis of the morphology of first-year sea ice ridges”, Cold Regions Science and Technology 82, pp 94 - 109.

Suominen, M. & Kujala, P., 2012, “Ice Model Tests in Compressive Ice”, 21st IAHR International Symposium on Ice, Dalian, China.

Timco, G. W. and Burden, R. P., 1997, “An Analysis of the Shapes of Sea Ice Ridges”, Cold Regions Science and Technology, Volume 25, pp 65 - 77.

Timco, G. W., Croasdale, K. and Wright, B., 2000, “An Overview of First-Year Sea Ice Ridges”, Canadian Hydraulics Centre, Technical Report HYD-TR-047, PERD/CHC Report 5-112, August

Wang, J., Sayeed, T. et al., 2016, “Ice Model Tests for Dynamic Positioning Vessel in Managed Ice”, In Proc. of the Arctic Technology Conference.

6. FUTURE WORK

1. Guidelines for tests with offshore structures –

2. Guideline for ice trials – It is suggested to prepare in principle a new guideline because the previous guideline cannot be considered applicable anymore as it is outdated. In. The guideline should include the performance of the tests, ice measurement practises and analysis methods.
3. Review on numerical methods to predict the performance of ships in ice in cooperation with ISSC.
4. Guideline or proposal for waves in ice, which is a topic gaining increasing attention.
5. Uncertainty analysis